Acta Cryst. (1987). A43, 825-836

Resolution Function of an X-ray Triple-Crystal Diffractometer

BY R. A. COWLEY

Department of Physics, University of Edinburgh, Mayfield Road, Edinburgh EH9 3JZ, Scotland

(*Received* 2 *June* 1987; *accepted* 13 *July* 1987)

Abstract

The resolution function of an X-ray triple-crystal diffractometer is calculated on the assumption that the resolution is controlled by the properties of the monochromating and analysing crystals. The expressions are then evaluated when these crystals have either a mosaic structure or when they are perfect flat crystals with a reflectivity controlled by the Darwin width. Within the Gaussian approximation for the Darwin curve, simple expressions for the resolution are then obtained both for a conventional X-ray source and for an X-ray synchrotron source, although the expressions differ in detail. The expressions are used to discuss the intensity obtained when a triple-crystal diffractometer is used to measure the integrated Bragg reflection intensity, the intensity associated with rods in reciprocal space and the intensity of diffuse scattering.

1. Introduction

Over the past few years X-ray scattering experiments have been performed to explore new areas in phase transitions and surface science. The high brilliance available with rotating-anode and synchrotron sources has enabled experiments to be performed with a momentum resolution of $\sim 10^{-4}$ Å^{-1}. These experiments have mostly used a three-axis spectrometer, Fig. 1, with perfect or nearly perfect crystals as monochromator and analyser. Despite the high resolution available with nearly perfect crystals, it is still necessary to understand the resolution function if detailed experiments are to be performed, if reliable information about intensities is to be obtained, and if improvements are to be made in the experiments.

The calculation of the resolution function of a neutron three-axis spectrometer has been carried through by several authors (Cooper & Nathans, 1967; Stedman, 1968; Bjerrum-Møller & Nielsen, 1970). The corresponding calculation for an X-ray three-axis diffractometer is in some ways simpler, and in other ways more difficult than for the neutron case. It is easier because only elastic scattering processes, in which the energy of the incident and scattered X-ray photons are the same, need to be considered. This is an excellent approximation for studies of the positions and motions of the atoms. The second simplification is that the beam divergences are largely controlled by the monochromator and analyser crystals, and not by Soller-slit collimators between the monochromator and detector, as they are in typical neutron experiments. In the X-ray case, slits are used to define the beams, but the resolution is only easily controlled if these slits do not control the angular divergence of the beams between the monochromator and analyser crystals at least in the scattering plane. If this is not the case the resolution becomes a complex interaction between real-space and reciprocal-space effects, and cannot be readily controlled or calculated.

In the neutron scattering case the resolution was calculated for mosaic crystals with a mosaic spread which is assumed to have a Gaussian form. With X-rays the monochromator and analyser are often perfect crystals and dynamical diffraction theory (Zachariasen, 1945) must be used to describe the reflection at the monochromator and analyser. The scattering profile obtained from the dynamical theory differs from that given by the kinematical theory firstly because it corresponds more closely to an uncertainty in the plane spacing, instead of from misaligned planes, and secondly because the line shape is not Gaussian. This latter effect creates a non-Gaussian resolution function with large $1/\theta^2$ tails which, in the dynamical scattering theory, arise from scattering by

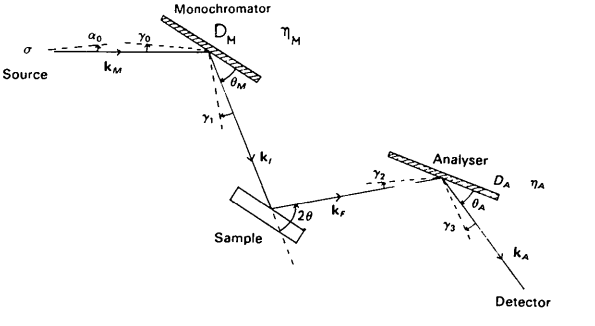

Fig. 1. A schematic diagram of the triple-crystal X-ray diffractometer in real space showing the directions of the nominal wave vectors $\mathbf{k}_M$, $\mathbf{k}_I$, $\mathbf{k}_F$, $\mathbf{k}_A$ and the deviations γ_0, γ_1, γ_2, γ_3 of a typical ray.

0108-7673/87/060825-12$01.50

the surface of the monochromator or analyser. These give rise to long tails to the resolution function in particular directions in wave-vector space. Avoiding these tails is essential if weak diffuse scattering is to be studied close to Bragg reflections, and the directions and origins of these tails are described in detail by Ryan (1986).

In this paper we are concerned not with the tails of the resolution function, but with the central part. This was calculated before by Pynn, Fujii & Shirane (1983) and in principle involves a complex numerical integration using the results of dynamical theory for both monochromator and analyser. In this paper we adopt a more pragmatic approach and, as suggested by Pynn *et al.* (1983), approximate the results of the dynamical theory by a Gaussian of the appropriate width, and then hope that after this has been convoluted with the other less-restrictive resolution elements, the Gaussian form is an adequate approximation. This has the advantage that we can then obtain detailed and relatively simple expressions for the resolution function, which are very useful in practice. In § 2 the expressions for the resolution function of a three-crystal diffractometer are obtained for both mosaic crystals and perfect crystals as monochromator and analyser. The former are useful when relaxed collimation or higher intensity is required. We also develop expressions for when the source is a line spectrum, from say a rotating-anode source, and when it has a continuous spectrum, as arises from a synchrotron source, in which case the pre-monochromator collimation determines the resolution. In this section we also give expressions for the variations in the intensity due to the polarization and absorption factors in the scattering cross section for a typical scattering geometry.

The result of an experiment is a convolution of the resolution function of the instrument with the scattering function, $S(Q)$, where Q is the wave-vector transfer in the experiment. In general this is a complicated integral, but there are several special cases which can be evaluated and which are of importance. One example is the determination of the intensity of Bragg reflections. The usual technique is to employ an open detector when the formulae for the integrated intensities are well known, but this is not the case when an analyser is used. The possible procedures and the relevant formulae for the integrated intensities are given in § 3. Another simple example which can be evaluated analytically is that of a line of scattering in reciprocal space. This case is also discussed in § 3.

In § 4 we show how the results obtained in § 2 are modified if more complex monochromators or analysers are used. In particular we discuss the resolution obtained when asymmetrically cut crystals and double monochromators are used. The results of the paper are summarized and discussed in a final section.

2. The resolution function

The calculation of the resolution function for an X-ray three-crystal spectrometer will follow the method and, as far as possible, the notation of Cooper & Nathans (1967). A schematic diagram of the idealized form of the spectrometer is shown in Fig 1, and a corresponding reciprocal-space diagram in Fig. 2. The spectrometer resolution is assumed to be controlled in the scattering plane by the monochromator and analyser crystals, which are further assumed to be symmetrically cut single crystals. Extensions to asymmetrically cut crystals and to double monochromators are discussed in § 4. In addition to the monochromator and analyser crystals, the resolution also depends on the wavelength spread of the X-rays. This is determined in an experiment with a conventional source by the line width of the X-ray line chosen, and in an experiment with a synchrotron source by the effective angular divergence between the monochromator and source.

The nominal wave vectors of the X-ray photons from source to detector $\mathbf{k}_M$, $\mathbf{k}_I$, $\mathbf{k}_F$ and $\mathbf{k}_A$ are all of equal magnitude k, and the nominal wave-vector transfer to the specimen is

$$\mathbf{Q}_0 = \mathbf{k}_I - \mathbf{k}_F, \quad |\mathbf{Q}_0| = 2k \sin\theta. \tag{2.1}$$

The corresponding wave vectors of a particular photon are $\mathbf{k}_m$, $\mathbf{k}_i$, $\mathbf{k}_f$ and $\mathbf{k}_a$, and deviate from the nominal ray by angles of γ_0, γ_1, γ_2 and γ_3 in the scattering plane, and by δ_0, δ_1, δ_2 and δ_3 out of the scattering plane. Since the energy of the X-ray photon is, within error, unchanged in these scattering experiments,

$$|\mathbf{k}_m| = |\mathbf{k}_i| = |\mathbf{k}_f| = |\mathbf{k}_a|.$$

The effect of a mosaic structure to the monochromator is that reflection will occur even if the angles of deviation from the nominal rays γ_0 and $-\gamma_1$ are unequal (Fig. 1), while for perfect crystals $\gamma_0 = -\gamma_1$,

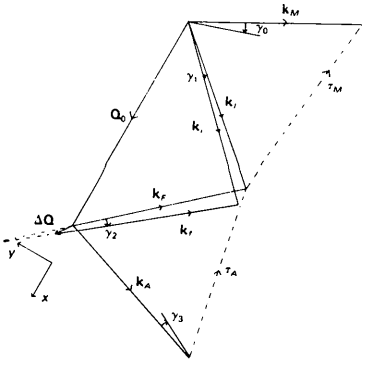

Fig. 2. A wave-vector space diagram of the triple-crystal diffractometer shown in Fig. 1. τ_M and τ_A are the wave-vector transfers to the monochromator and analyser and $\mathbf{Q}_0$ the wave-vector transfer to the sample.

and the reflectivity is determined by the dynamical theory, which for thick non-absorbing crystals gives

$$\begin{aligned} P(y) &= 1 & |y| &< 1 \\ P(y) &= y-(y^2-1)^{1/2} & |y| &> 1 \end{aligned} \tag{2.2}$$

where

$$y=[\gamma_1-\gamma_0+(2\Delta k/k)\tan\theta_M]/2D_M. \tag{2.3}$$

$2D_M$ is the Darwin width of the reflection (Zachariasen, 1945) and $\Delta k=|\mathbf{k}_m|-|\mathbf{k}_M|$. Although, as explained by Pynn *et al.* (1983), the calculation of the resolution function can be performed with the Darwin function, it is then necessary to make numerical calculations for each specific case. A less-accurate but more tractable approach is to approximate (2.2) by a Gaussian form, when the reflectivity of the monochromator is given by

$$\begin{aligned} P(\gamma_0,\gamma_1,\Delta k) = P_M \exp\{-\tfrac{1}{2}[(\gamma_0+\gamma_1)/2\eta_M]^2\} \\ \times\exp(-\tfrac{1}{2}\{[\gamma_1-\gamma_0 \\ +2\Delta k(\tan\theta_M)/k]/2D_M\}^2), \end{aligned} \tag{2.4}$$

and the corresponding expression for the analyser is

$$\begin{aligned} P(\gamma_2,\gamma_3,\Delta k) = P_A \exp\{-\tfrac{1}{2}[(\gamma_2+\gamma_3)/2\eta_A]^2\} \\ \times\exp(-\tfrac{1}{2}\{[\gamma_2-\gamma_3 \\ -2\Delta k(\tan\theta_A)/k]/2D_A\}^2). \end{aligned} \tag{2.5}$$

These expressions emphasize the difference between the diffraction of mosaic crystals when effectively $D_M\to 0$ and $\gamma_0=\gamma_1+(2\Delta k/k)\tan\theta_M$, and ideal crystals when $\eta_M\to 0$ and $\gamma_0=-\gamma_1$. Although in principle it is possible to carry through the calculations with the full expressions for the reflectivity of monochromator and analyser [(2.4) and (2.5)], the resulting formulae are complicated. We shall therefore make use of the two limits which are most frequently of use in practice; of either ideal crystals such as flat Si or Ge monochromators for which $\eta_M<D_M$, and mosaic crystals such as bent Si or Ge or graphite crystals for which $\eta_M>D_M$.

In addition to the contribution to the resolution from the monochromator and analyser, there is also the effect of the line width of the X-ray source for conventional-source experiments. The probability of different wavelengths is independent of the angles γ_0 and δ_0 but is sharply peaked in wave vector near k_M. We shall therefore write the normalized wave-vector dependence of the source as

$$P_s(\Delta k)=(2\pi)^{-1/2}(k\sigma)^{-1}\exp[-\tfrac{1}{2}(\Delta k/k\sigma)^2], \tag{2.6}$$

where σ is given by the line width of the characteristic X-ray line.

If the source is a synchrotron, the resolution is determined at least in part by the emittance of the synchrotron source and the effective collimation between the synchrotron and the monochromator. These are assumed to have a Gaussian form

$$P_s=\exp[-\tfrac{1}{2}(\gamma_0^2/\alpha_0^2+\gamma_0^2/\beta_0^2)], \tag{2.7}$$

and similar expressions are used for the out-of-plane collimations between the monochromator and detector as defined by angles β_1, β_2 and β_3. We have now defined all the resolution elements of the spectrometer, and can use the method of Cooper & Nathans (1967) to evaluate the resolution function.

The in-plane resolution function

In the Gaussian approximation the resolution function of the triple-crystal spectrometer for a wave-vector transfer $\mathbf{Q}_0$ is given by a Gaussian form

$$\begin{aligned} R(\mathbf{Q}_0+\Delta\mathbf{Q}) = R_0\exp[-\tfrac{1}{2}(M_{12}\,\Delta Q_x^2+2M_{12}\,\Delta Q_x\,\Delta Q_y \\ +M_{22}\,\Delta Q_y^2+M_{33}\,\Delta Q_z^2)], \end{aligned} \tag{2.8}$$

where ΔQ_x is the component of the resolution function parallel to $\mathbf{Q}_0$, ΔQ_z is the component out of the scattering plane, and ΔQ_y is the third orthogonal component, as defined in Fig. 2. The contributions to the in-plane and out-of-plane resolution function are quite separate, and so in this subsection we discuss only the in-plane terms and their contribution to R_0 and leave to the next subsection the out-of-plane terms.

The in-plane contributions to the scale factor R_0 are (Chesser & Axe, 1973)

$$R_I=P_MP_AJR_{0x}, \tag{2.9}$$

where P_M and P_A are the efficiencies of monochromator and analyser. J is the Jacobian of the transformation from angles γ_1 and γ_2 to ΔQ_x and ΔQ_y, $J=(k^2\sin 2\theta)^{-1}$, and R_{0x} arises from performing the integral over Δk and is

$$R_{0x}=(2\pi k\sigma)^{-1}(A')^{-1/2} \tag{2.10}$$

for a continuous source, while A' depends on the resolution and angle of scattering as specified below. The expressions for the parameters A', M_{11}, M_{12} and M_{22} can now be evaluated for various configurations.

(*a*) *Conventional source - perfect crystals.*

$$\begin{aligned} A' = (\tan\theta-\tan\theta_A)^2/D_A^2+(\tan\theta-\tan\theta_M)^2/D_M^2 \\ +1/\sigma^2 \end{aligned} \tag{2.11}$$

$$\begin{aligned} M_{11} &= (4A'k^2\cos^2\theta)^{-1}(M_{11}^x+M_{11}^c) \\ M_{12} &= (4A'k^2\cos\theta\sin\theta)^{-1}(M_{12}^x+M_{12}^c) \\ M_{22} &= (4A'k^2\sin^2\theta)^{-1}(M_{22}^x+M_{22}^c), \end{aligned} \tag{2.12}$$

where M_{11}^x depends solely on the properties of the monochromator and analyser, and M_{11}^c on the line width of the source. The detailed expressions for the

M^x terms are

$$\begin{aligned} M^x_{11} &= (\tan\theta_M - \tan\theta_A)^2/D_M^2 D_A^2 \\ M^x_{12} &= (\tan\theta_M - \tan\theta_A) \\ &\quad \times (2\tan\theta - \tan\theta_M - \tan\theta_A)/D_M^2 D_A^2 \\ M^x_{22} &= (2\tan\theta - \tan\theta_M - \tan\theta_A)^2/D_M^2 D_A^2, \end{aligned} \tag{2.13}$$

while the corresponding expressions for the dependence on the line width σ of the source are

$$\begin{aligned} M^c_{11} &= M^c_{22} = (1/D_A^2 + 1/D_M^2)/\sigma^2 \\ M^c_{12} &= (1/D_M^2 - 1/D_A^2)/\sigma^2. \end{aligned} \tag{2.14}$$

These results are further simplified if the monochromator and analyser are identical and used in the focusing configuration $\theta_M = \theta_A$ (Fig. 1), when

$$M^x_{11} = M^x_{12} = M^c_{12} = 0.$$

The resolution function then has its principal axis parallel and perpendicular to $\mathbf{Q}_0$, and furthermore the expression for M^c_{11} is independent of $\mathbf{Q}_0$ or θ and directly proportional to $1/\sigma^2$. The resolution is especially good when, in addition, $\theta = \theta_M$. In this case $A' = 1/\sigma^2$ and $M^x_{22} = 0$, while $M^c_{11} = M^c_{22} = 2/\sigma^2 D_M^2$. The resolution is then given by

$$M_{11} = [2D_M^2(\cos^2\theta)k^2]^{-1}$$

and

$$M_{22} = [2D_M^2(\sin^2\theta)k^2]^{-1}.$$

Both of these are independent of the line width σ, as is well known for the perfectly focusing geometry.

(*b*) *Conventional source - mosaic crystals.* In this case the expressions for the elements of the resolution function are identical with those for perfect crystals, except that η_M replaces D_M, and η_A replaces D_A. This is because the monochromator for a given direction of the beam incident on the specimen, γ_1, gives rise to different incident directions γ_0 for mosaic and perfect crystals. Since, however, there is no effective collimation before the monochromator or after the analyser, the resolution is of the same functional form in both cases but with η_M and η_A replacing D_M and D_A.

(*c*) *Synchrotron source - perfect crystals.*

$$\begin{aligned} A' &= (\tan\theta - \tan\theta_A)^2/D_A^2 + (\tan\theta - \tan\theta_M)^2/D_M^2 \\ &\quad + (1/\alpha_0^2)\tan^2\theta. \end{aligned} \tag{2.15}$$

The expressions for M_{11}, M_{12} and M_{22} are similar to those of (2.12)-(2.14) except that

$$\begin{aligned} M^c_{11} &= [(\tan^2\theta_M/D_M^2) + (\tan^2\theta_A/D_A^2)]/\alpha_0^2 \\ M^c_{12} &= [(\tan^2\theta_M/D_M^2) \\ &\quad + \tan\theta_A(\tan\theta_A - \tan\theta)/D_A^2]/\alpha_0^2 \\ M^c_{22} &= [(\tan^2\theta_M/D_M^2) + (2\tan\theta - \tan\theta_A)^2/D_A^2]/\alpha_0^2. \end{aligned} \tag{2.16}$$

These expressions are only slightly simplified in a symmetric arrangement with $\theta_M = \theta_A$ and $D_M = D_A$. The resolution function in this case does not have one of its principal axes parallel to $\mathbf{Q}_0$, because M^c_{12} is in general non-zero. Nevertheless, since α_0^2 is usually large compared with D_M^2, by far the largest component of the M's is M^x_{22}, unless $\theta = \theta_M$. Consequently one of the principal axes of the resolution matrix will be at least approximately along $\mathbf{Q}_0$.

(*d*) *Synchrotron source - mosaic crystals.*

$$\begin{aligned} A' &= (\tan\theta - \tan\theta_A)^2/\eta_A^2 + (\tan\theta - \tan\theta_M)^2/\eta_M^2 \\ &\quad + (\tan\theta - 2\tan\theta_M)^2/\alpha_0^2 \end{aligned} \tag{2.17}$$

$$\begin{aligned} M^c_{11} &= [(2\tan\theta_M - \tan\theta_A)^2/\eta_M^2 + (\tan^2\theta_M)/\eta_M^2]/\alpha_0^2 \\ M^c_{12} &= \{4(\tan^2\theta_A - \tan^2\theta_M)/\alpha_0^2 \\ &\quad + [\tan\theta_A(\tan\theta_A - 2\tan\theta) \\ &\quad + 4\tan\theta_M(\tan\theta - \tan\theta_M)]/\eta_A^2 \\ &\quad + (\tan^2\theta_M)/\eta_M^2\}/\alpha_0^2 \\ M^c_{22} &= [(2\tan\theta - 2\tan\theta_M - \tan\theta_A)^2/\eta_A^2 \\ &\quad + (\tan^2\theta_M)/\eta_M^2]/\alpha_0^2. \end{aligned} \tag{2.18}$$

If a symmetric configuration is used then the expressions are somewhat simpler:

$$\begin{aligned} M^c_{11} &= 2(\tan^2\theta_M)/\alpha_0^2\eta_M^2 \\ M^c_{12} &= 2(\tan\theta_M)(\tan\theta - \tan\theta_M)/\alpha_0^2\eta_M^2 \\ M^c_{22} &= 2(2\tan^2\theta + 5\tan^2\theta_M - 6\tan\theta\tan\theta_M)/\alpha_0^2\eta_M^2. \end{aligned} \tag{2.19}$$

As with the perfect crystals, the resolution matrix does not have one of its principal axes along $\mathbf{Q}_0$.

Although these derivations have been given with either perfect or mosaic crystals for both monochromator and analyser crystal, the results can readily be generalized to apply to experiments with one of each. In the case, for example, of a perfect monochromator but mosaic analyser, the results are given by (2.11)-(2.16) of parts (*a*) or (*c*) but with D_A replaced by η_A.

The out-of-plane resolution

The resolution of the X-ray triple-crystal spectrometer perpendicular to the scattering plane is identical to that of the neutron spectrometer. We can therefore take over the results of Cooper & Nathans (1967) as corrected, for example, by Chesser & Axe (1973). The contribution to the scale factor R_0 is R_V, where

$$\begin{aligned} R_V &= [(2\pi)^{1/2}/k]\{\beta_0^2/[\beta_0^2 + (2\eta'_M\sin\theta_M)^2]\}^{1/2} \\ &\quad \times \{\beta_3^2/[\beta_3^2 + (2\eta'_A\sin\theta_A)^2]\}^{1/2}(a_{11} + a_{12})^{-1/2}. \end{aligned} \tag{2.20}$$

The out-of-plane collimations are $\beta_0, \ldots \beta_3$, and the out-of-plane mosaic spread of the monochromator

and analyser are η'_M and η'_A respectively, and are zero if the crystals are perfect. The factors a_{11} and a_{12} are given by

$$a_{11} = [4(\eta'_M)^2 \sin\theta_M^2 + \beta_0^2]^{-1} + \beta_1^{-2}$$

and (2.21)

$$a_{12} = [4\sin^2\theta_A(\eta'_A)^2 + \beta_3^2]^{-1} + \beta_2^{-2}.$$

The out-of-plane element of the resolution matrix, M_{33} of (2.8), is

$$M_{33} = (1/k^2)a_{11}a_{12}/(a_{11}+a_{12}). \quad (2.22)$$

It is very frequently the case that the mosaic spreads η'_A and η'_M are negligible when

$$R_V = (2\pi/k)^{1/2}(1/\beta_0^2 + 1/\beta_1^2 + 1/\beta_2^2 + 1/\beta_3^2)^{-1/2}$$

and

$$M_{33} = \frac{(\beta_0^{-2}+\beta_1^{-2})(\beta_2^{-2}+\beta_3^{-2})}{k^2(\beta_0^{-2}+\beta_1^{-2}+\beta_2^{-2}+\beta_3^{-2})}.$$

These results are simpler than the in-plane resolution in that they are independent of the angle of scattering, θ, and constant for a given spectrometer configuration.

Polarization and absorption

The radiation emitted by a conventional source is unpolarized, and so it is necessary to consider the components of the polarization both in and perpendicular to the scattering plane. The polarization dependence of electric dipole scattering then gives a factor of one for the out-of-plane polarization and a reduced factor for the in-plane component so that the total polarization factor is

$$R_p = (1+\cos^2 2\theta_M \cos^2 2\theta \cos^2 2\theta_A)/2. \quad (2.23)$$

When perfect crystals are used polarization effects also influence the reflectivity of the monochromator and analyser. The Darwin widths, D_M and D_A, are dependent upon the polarization, and are reduced by $\cos 2\theta_M$ and $\cos 2\theta_A$ for the in-plane component compared with their values for the out-of-plane component. This means that the intensity is given by two superimposed components with different widths, and whose intensities are given by $\frac{1}{2}$ for the out-of-plane polarization and by the product of cosine factors for the in-plane component. If, furthermore, the monochromator or analyser are not cubic crystals, the X-ray refractive index for the two polarization components is different, giving slightly different Bragg angles, and so the centres of the two resolution functions are slightly displaced from one another. Clearly it is not advisable to use very anisotropic crystals as monochromators or analysers.

The beam from a synchrotron is polarized in the plane of the direction in which the electrons have been accelerated, usually horizontal. The spectrometer is then preferably aligned vertically when only the out-of-plane polarization component is present and there are no polarization corrections, $R_p = 1$. Sometimes it is more convenient for the spectrometer to be aligned in the horizontal plane, when the appropriate expressions are those of the in-plane polarization component,

$$R_p = \cos^2 2\theta_M \cos^2 2\theta \cos^2 2\theta_A. \quad (2.24)$$

In neither case, however, are there the complications arising from the two resolution functions of different widths which occur for a conventional source.

The effect of absorption in the sample on the scattered intensity is dependent upon the size and geometry of both the incident beam and the sample crystal. Experimentally we find it is most convenient in these experiments to use the extended-face geometry, in which the sample has a large flat face which intersects the whole of the incident beam. The sample is also sufficiently thick that the incident beam is wholly absorbed in the sample. The effect of the absorption is then to modify the intensity by the factor

$$R_A = \sin(2\theta-\psi)/[\sin\psi + \sin(2\theta-\psi)], \quad (2.25)$$

where ψ is the angle in the scattering plane between the direction of the incident beam and the flat face of the sample. The angular dependence arises because when the incident X-ray beam propagates in the crystal close to the surface, ψ small, the scattered beam more readily escapes from the sample than if the scattering occurred at considerable depth in the crystal.

X-ray experiments can also be used to study thin films and surface effects. In these cases the intensity is proportional to the area of the surface illuminated by the X-ray beam, which is dependent upon the angle ψ between the incident beam and the surface,

$$R_s = (\sin\psi)^{-1}. \quad (2.26)$$

Of course, when ψ becomes small the illuminated length of surface is very large, and extremely long samples must be used if (2.26) is to be correct.

3. Resolution widths and intensities

Resolution widths

The resolution in the scattering plane is defined by the locus of ΔQ_x and ΔQ_y such that

$$0{\cdot}5 = \exp[-\tfrac{1}{2}(M_{11}\Delta Q_x^2 + 2M_{12}\Delta Q_x \Delta Q_y + M_{22}\Delta Q_y^2)].$$

In the case of a conventional source with a symmetric arrangement of monochromator and analyser $M_{12} =$

0, and the resolution is defined by (FWHM)

$$\Delta_x = 2[2(\ln 2)/M_{11}]^{1/2}$$
$$= 4k \cos\theta[2A' \ln 2/(M_{11}^x + M_{11}^c)]^{1/2} \quad (3.1)$$

and

$$\Delta_y = 2[2(\ln 2)/M_{22}]^{1/2}$$
$$= 4k \sin\theta[2A' \ln 2/(M_{22}^x + M_{22}^c)]^{1/2},$$

while the θ dependence of the scale factor, R_0, is contained in the factor

$$I_s = 1/\sin 2\theta(A')^{1/2}. \quad (3.2)$$

These expressions have been calculated as a function of Q_0, and the results are shown in Figs. 3-5. In Fig. 3 the parameters are chosen for a Cu $K\alpha_1$ source, $\lambda = 1{\cdot}5405$ Å, $\sigma = 3{\cdot}5 \times 10^{-4}$ (FWHM) and for a Si(111) monochromator and analyser with a Darwin width $D_M = 33{\cdot}6$ μrad (FWHM). The results show that the longitudinal resolution width Δ_x is approximately ten times the transverse width, that both increase for large Q_0, but that Δ_x has a minimum at the focusing position when $\theta = \theta_M$.

In Fig. 4 the monochromator and analyser are chosen to have mosaic spreads of 0·02°, 0·35 mrad (FWHM). The effect of this is to make the resolution function more symmetrical at least for larger Q_0 with Δ_x approximately independent of Q_0. Δ_x is barely any larger at large Q_0 than with the perfect crystals (Fig. 3) but Δ_y is roughly ten times larger for all Q_0.

In the calculations shown in Fig. 5 the mosaic spread was increased to 0·2°, 3·5 mrad (FWHM) so that the conditions are characteristic of those when pyrolytic graphite crystals are used. Δ_y has a similar form to that shown in Figs. 3 and 4 but is ten times larger again. Δ_x now decreases with increasing Q_0 and at larger $Q_0 > 5$ Å^{-1} is smaller than Δ_y.

Similar calculations for a synchrotron source with a small angular emittance for a synchrotron of 0·2 mrad (FWHM) are shown in Figs. 6-8. The expressions are more complicated, because M_{12} is

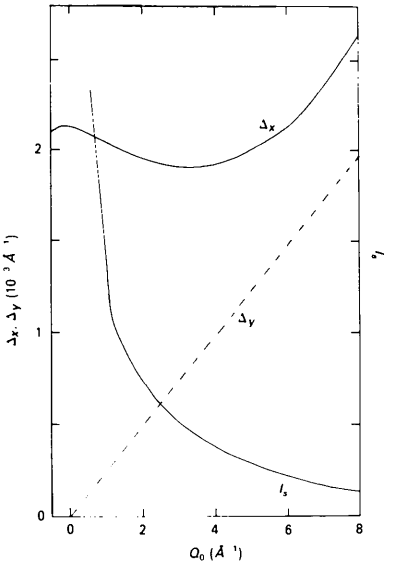

Fig. 4. The resolution function, as in Fig. 3, except that the monochromator and analyser have mosaic spreads (FWHM) of 0·02°.

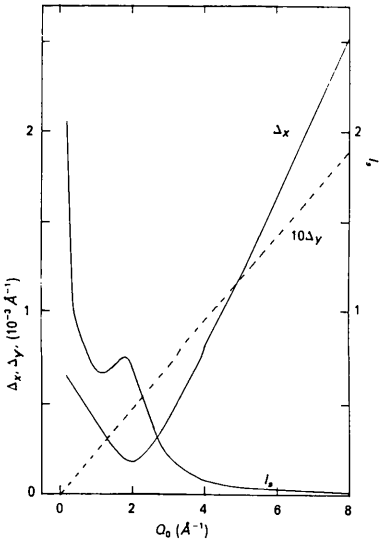

Fig. 3. The width (FWHM) of the resolution function for Cu $K\alpha_1$ radiation, $\lambda = 1{\cdot}54$ Å, and Si(111) monochromator and analyser, $D_M = 0{\cdot}002°$ (FWHM). Δ_x is the width parallel to $\mathbf{Q}_0$, Δ_y the perpendicular width and I_s the angular dependence of the scale factor.

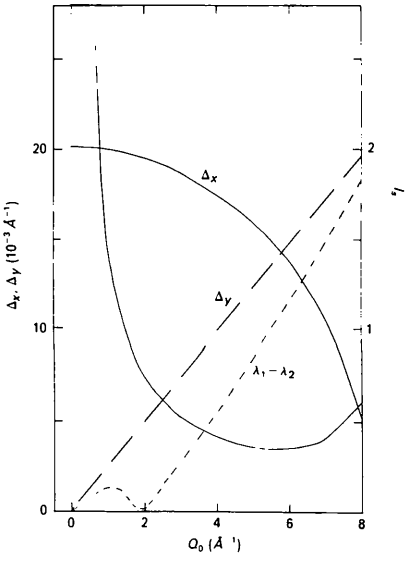

Fig. 5. The resolution function, as in Fig. 3, except that the monochromator and analyser have mosaic spreads (FWHM) of 0·2°. The $\lambda_1 - \lambda_2$ line gives the separation along $\mathbf{Q}_0$ of Cu $K\alpha_1$ and $K\alpha_2$ lines.

non-zero, and so the principal axes of the resolution function are not parallel and perpendicular to $\mathbf{Q}_0$. We have therefore calculated Δ_1 and Δ_2 as the principal axes of the resolution ellipse, and β is the angle between Δ_1 and $\mathbf{Q}_0$.

Fig. 6 shows the calculations for an Si(111) monochromator and analyser. The angle β is always very small, which shows that the resolution ellipse is oriented largely along $\mathbf{Q}_0$. Δ_2 is very similar to Δ_y of Fig. 3 because the transverse resolution is largely controlled by the monochromator and analyser. The longitudinal resolution Δ_1 is similar to Δ_x at the focusing wave vector $\theta = \theta_M$ ($Q_0 = 2$ Å^{-1}) but is approximately $2\frac{1}{2}$ times larger with the synchrotron source than with the conventional source. This is because the angular emittance of the synchrotron allows a larger spread in Δk from the monochromator than that provided by the line width of the Cu $K\alpha_1$ conventional source. If a larger angle at the monochromator was used, say Si(333) planes, the resolutions would be very similar for a synchrotron and a conventional source.

Figs. 7 and 8 show the corresponding calculations for mosaic crystals with $\eta_M = 0{\cdot}35$ and $3{\cdot}5$ mrad (FWHM). The results show that the principal axes of the resolution function are dependent on Q_0. In both cases, the width largely transverse to Q_0 is roughly comparable to that obtained from a conventional source, while the largely longitudinal width is much greater. The scale factor I_s is also very strongly peaked as a function of Q_0.

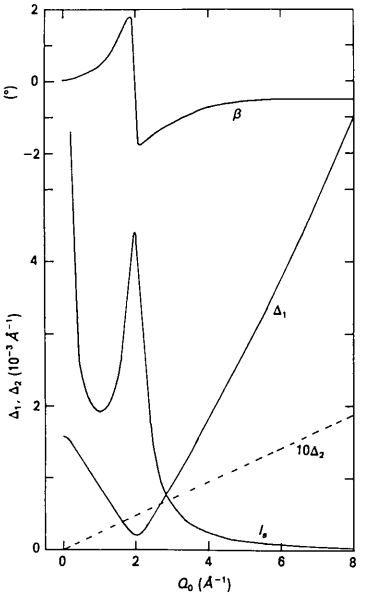

Fig. 6. The resolution function with a continuous source with pre-monochromator collimation of 0·012° FWHM and $\lambda = 1{\cdot}5$ Å. Δ_1 and Δ_2 are the widths (FWHM) of the principal axes and β the angle between Δ_1 and $\mathbf{Q}_0$. I_s is the angular-dependent scale factor. The monochromator and analyser are Si (111) planes, $D_M = 0{\cdot}002°$ (FWHM).

Measurement of Bragg reflection intensities

The relative intensities of the Bragg reflections provide information about the crystal structure of the sample. Suppose the scattering cross section is given by

$$S(\mathbf{Q}) = F_B \delta(\mathbf{Q} - \boldsymbol{\tau}), \tag{3.3}$$

where $\boldsymbol{\tau}$ is a reciprocal-lattice vector of the sample.

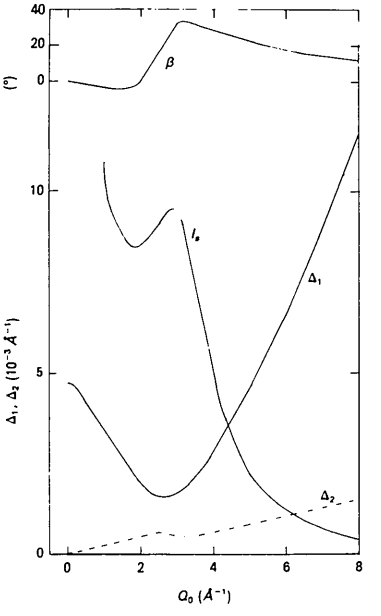

Fig. 7. The resolution function, as in Fig. 6, except that the monochromator and analyser have mosaic spreads of 0·02°.

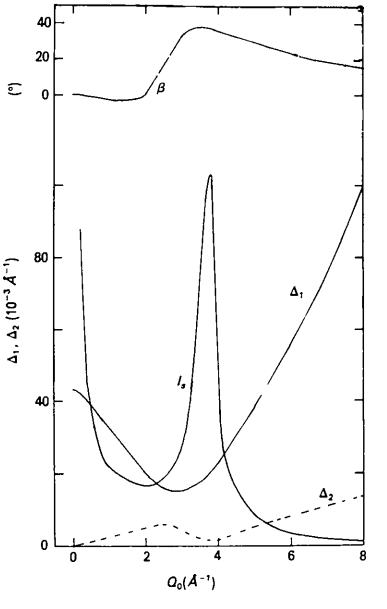

Fig. 8. The resolution function, as in Fig. 6, except that the monochromator and analyser have mosaic spreads of 0·2°.

One way of determining the structure factors F_B is to record the intensity when the spectrometer is set with $Q_0 = \tau$. The intensity is then given by all the amplitude factors

$$I_P(\tau) = R_I R_V R_P R_A F_B. \quad (3.4)$$

The dependence of the intensity on the polarization and absorption factors R_P and R_A [(2.23)-(2.25)] are easily evaluated, while R_V [(2.20)] is independent of the scattering angle. The factor R_I [(2.9)] is, however, more complicated, and depends simply on 2θ through the J factor and in a much more complex way through R_{0x} and A'. The latter is particularly complicated, and, as shown in Figs. 3-8, the θ dependence is dependent on the resolution of the spectrometer and varies rapidly with θ. This way of determining the intensities F_B is also unsatisfactory because it is difficult to find the maximum intensity.

The usual method of determining the Bragg structure factors is by measuring the integrated intensity when the spectrometer is controlled so as to sweep the resolution function through the Bragg reflection. In the study of crystals with incommensurate modulations of the basic structure, it is convenient to observe the intensities of the incommensurate satellites by scanning the wave-vector transfer Q_0 along the lines in reciprocal space parallel to the incommensurate wave vector. If the angle between the scanning direction and the wave-vector transfer is α, the integrated intensity is

$$I_1(\tau) = (2\pi)^{1/2} R_I R_V R_P R_A M^{-1/2} F_B, \quad (3.5)$$

where

$$M = M_{11}\cos^2\alpha + 2M_{12}\cos\alpha\sin\alpha + M_{22}\sin^2\alpha.$$

This expression is far from simple and depends on both θ and the resolution elements. Clearly such measurements can only be quantitatively analysed to obtain the intensities F_B for a wide range of different reciprocal-lattice points τ, if very careful and detailed resolution calculations are performed to correct for the θ and α dependence of $I_1(\tau)$.

The results do simplify if $\alpha = 0°$ when the scanning direction is parallel to $\mathbf{Q}_0$, because $M_{11}^x + M_{11}^c$ is independent of θ [(2.13), (2.14) and (2.16)]. The integrated intensity of the Bragg reflections is then given by

$$I_x(\tau) = P_M P_A R_I R_P R_A R_V \times 2k(\cos\theta)A'(M_{11}^x + M_{11}^c)^{-1/2} F_B, \quad (3.6)$$

where, in the case of perfect crystals and a conventional source, (2.13) and (2.14) give

$$M_{11}^x + M_{11}^c = (\tan\theta_M - \tan\theta_A)^2/D_M^2 D_A^2 + (1/D_A^2 + 1/D_M^2)/\sigma^2, \quad (3.7)$$

which is independent of angle θ. This is therefore the most satisfactory way to measure the relative intensities, F_B, as the dependence on θ does not depend on the resolution function, because the A' cancels the A' in the factor R_I. It is worth commenting that this result is a particular case of a more general result, that even if the triple-crystal spectrometer has significant collimation between the sample and the analyser, or the analyser and the detector, the θ dependence of the relative intensities measured with a scan for which $\alpha = 0$ is given by $(\sin\theta)^{-1} R_P R_A$. This result is similar to the well known result for a $\theta/2\theta$ scan of a two-crystal diffractometer, except that the integrated intensity is usually expressed as an integral over θ; since $\mathrm{d}Q_x = 2k\cos\theta\,\mathrm{d}\theta$, the intensity integrated over the angle θ is given by (3.6) divided by $2k\cos\theta$, which is then equivalent to the usual expression.

When the spectrometer has perfect crystals for the monochromator and analyser, the above procedure is difficult to follow because of the necessity of having the good transverse resolution, Figs. 3 and 6, aligned so that the scan of $\mathbf{Q}_0$ passes exactly through the Bragg reflection, and indeed the integral is incorrect if the sample has a mosaic spread larger than this narrow resolution width (Axe & Hastings, 1983). It is therefore more convenient to integrate the Bragg-reflection intensity by scanning along the transverse direction $\mathbf{Q}_y$. The resulting variation in the integrated intensity is then given for a conventional source by

$$I_y(\tau) = [P_M P_A R_P R_A R_V/(2\pi)^{1/2}\sigma k^2\cos\theta] \times (M_{22}^x + M_{22}^c)^{-1/2} F_B. \quad (3.8)$$

This expression depends on θ in a more complex way than that obtained if the diffractometer was used in the conventional manner with an open detector. Equation (3.8) is compared with that obtained with an open detector in Figs. 9 and 10. Both spectrometers are assumed to have the same vertical collimation and we have omitted the polarization and absorption corrections and taken $P_A = 1$. The results for a conventional source, Fig. 9, show a very marked difference in the intensities when the analyser has a small Darwin width or small mosaic spread, but the relative intensities are at least roughly constant when an analyser with a broad mosaic spread is used.

The results obtained for a continuous synchrotron source show the ratio of the intensities is a strongly peaked function of $|\mathbf{Q}_0|$ for a perfect analyser and that this peak only slowly broadens as the mosaic width of the monochromator and analyser increases.

Figs. 9 and 10 show very marked variations in intensity as a function of Q_0. Clearly these corrections are essential if the structure factors F_B are to be reliably measured with transverse scans.

An alternative approach, which is by far the most satisfactory, is to measure the integrated Bragg reflection by performing a double integral over Q_x and Q_y. There are then no errors due to possible inadequate

alignment of the spectrometer, and more significantly the result includes the effects of the dynamical broadening of the sample Bragg reflections as well as any mosaic effects. The integrated intensity is then given by

$$I_{xy}(\tau) = 2\pi R_I R_V R_P R_A (M_{11}M_{22} - M_{12}^2)^{-1/2} F_B. \quad (3.9)$$

For a conventional X-ray source, this can be simplified by the use of (2.11)-(2.14) to give

$$I_{XY}(\tau) = R_V R_P R_A (P_M P_A / k\sigma) D_A D_M F_B.$$

This result is independent of θ apart from the polarization and absorption factors R_P and R_A. The corresponding result for a synchrotron source with perfect crystals as monochromator and analyser is

$$I_{xy}(\tau) = (2\pi)^{1/2} R_V R_P R_A P_M P_A \times (\alpha_0 D_A D_M F_B / \tan\theta_M), \quad (3.10)$$

and with mosaic crystals

$$I_{xy}(\tau) = \pi^{1/2} R_V R_P R_A P_A P_M (\alpha_0 \eta_A / \tan\theta_M) \times (1/\eta_M^2 + 1/\alpha_0^2)^{-1} F_B. \quad (3.11)$$

Both of these results are similar to those for a conventional source, in that they are independent of θ apart from the absorption and possibly the polarization corrections.

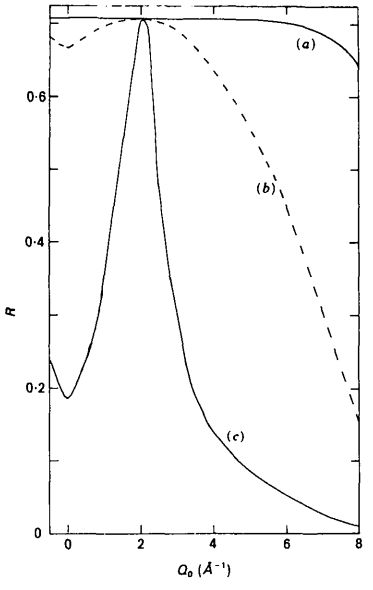

Fig. 9. The ratio of the integrated intensity observed in a transverse scan across a Bragg reflection to that observed with an open detector, as a function of wave-vector transfer. The incident wave vector is Cu $K\alpha_1$ and the monochromator and analyser are varied with (*a*) $D_M = 0{\cdot}002$, (*b*) $\eta_M = 0{\cdot}02$ and (*c*) $\eta_M = 0{\cdot}2°$.

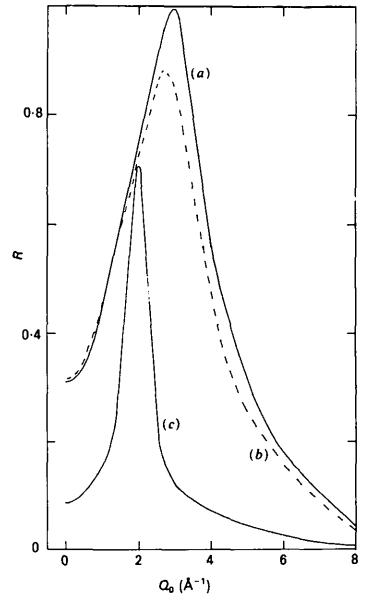

Fig. 10. The ratio of the integrated intensity observed in a transverse scan across a Bragg reflection to that observed with an open detector. The source is assumed to be continuous with a pre-monochromator collimation of 0·012° (FWHM), $\lambda = 1{\cdot}5°$. The results are shown for different monochromator and analyser crystals; (*a*) $D_M = 0{\cdot}002$, (*b*) $\eta_M = 0{\cdot}02$ and (*c*) $\eta_M = 0{\cdot}2°$.

Intensity from a rod of scattering

Triple-crystal X-ray diffractometers are particularly suited to study the scattering from surfaces and interfaces. They have been used to study the scattering from ferroelectric domain walls (Andrews & Cowley, 1986), the scattering arising near Bragg reflections from the termination of the crystal lattice (Andrews & Cowley, 1985; Robinson, 1986), and the *X*-ray reflectivity of surfaces (Cowley & Ryan, 1987). In all of these cases the scattering is confined to a line in reciprocal space perpendicular to the interface, and relatively slowly varying in intensity along the scattering rod. If these rods are aligned in the scattering plane, the intensity when the spectrometer is set with a wave vector $\mathbf{Q}_0$ on the rod is given by a one-dimensional integral over the resolution function and along the direction of the rod. If the intensity along the rod can be treated as constant this intensity is the $I_1(Q_0)$ of (3.5), with α the angle between $\mathbf{Q}_0$ and the rod of scattering. This result is, however, dependent on the scattering geometry in a complex way. It is experimentally more satisfactory to measure the integrated intensity by varying the wave vector transversely through the rod of scattering. The integrated intensity is then given by $I_{xy}(Q_0)$ [(3.9)-(3.11)], provided that the interfaces are uniformly distributed throughout the volume of the sample, as indeed they may be for ferroelectric domain walls. As explained above, this result then depends on the scattering geometry only through the polarization and absorption factors R_A and R_P, and there is no Lorentzian factor as assumed by Robinson, Waskiewicz, Teng & Bohr (1986).

In many experiments the interface of interest is the surface of the crystal, and then the absorption correction is inapplicable but is replaced by the surface factor R_s of (2.27). This factor is of special importance when ψ is small, as it is when the reflectivity curve is being determined for small angles θ. The Fresnel formula for the X-ray reflectivity gives at angles θ much larger than the critical angle θ_c a reflectivity proportional to θ^{-4}. This angular factor arises in the kinematical theory of X-ray diffraction because the Fourier transform of a step or sharp surface electron density profile is proportional to θ^{-2}. With a symmetric geometry $\psi = \theta$ and the surface factor $R_s = \theta^{-1}$. Finally, the Fresnel derivation of the reflectivity assumes that the sample is scanned in angle rather than transverse wave vector, when $Q_y = 2k\theta\,\Delta\psi$, giving a further factor of θ^{-1} for the integrated intensity observed by scanning through the rod in constant angular steps.

The diffuse scattering

One of the applications of the triple-crystal spectrometer is the study of diffuse scattering. If this scattering has a uniform structure factor S_0 over the volume of the resolution function the observed intensity is

$$I_{xyz}(\mathbf{Q}_0) = I_{xy}(\mathbf{Q}_0)(R_W/R_V)S_0, \qquad (3.12)$$

where R_W is the integral over the vertical resolution function

$$R_W = 2\pi\beta_0\beta_1\beta_2\beta_3[\beta_1^2+\beta_0^2+4(\eta'_M)^2\sin^2\theta_M]^{-1/2} \times[\beta_2^2+\beta_3^2+4(\eta'_A)^2\sin^2\theta_A]^{-1/2}. \qquad (3.13)$$

This result is independent of θ apart from the absorption, R_A, and polarization, R_P, corrections.

4. Other monochromators

Asymmetrically cut monochromators

The use of asymmetrically cut monochromators enables the beam to be reduced or expanded in width. Although this feature does not alter the resolution in reciprocal space, the resolution is altered in the case of perfect crystals by the changed relationship in the dynamical theory between the deviation angles γ_0 and γ_1. For symmetrically cut perfect crystals $\gamma_0 = -\gamma_1$ [(2.4)], because the deviation in the wave-vector transfer to the monochromator is perpendicular to the surface of the crystal, which for symmetrically cut crystals is parallel to the reflecting planes. When the crystal is asymmetrically cut so that the reflecting planes are at an angle ψ_M to the surface of the crystal, and the angle of incidence to the surface is $\theta_M - \psi_M$, the corresponding relation between ψ_0 and ψ_1 is (Zachariasen, 1945)

$$\gamma_0 = -\left(\frac{\tan\theta_M - \tan\psi_M}{\tan\theta_M + \tan\psi_M}\right)\gamma_1 + \frac{2\Delta k}{k}\frac{\tan\theta_M\tan\psi_M}{(\tan\theta_M+\tan\psi_M)}. \qquad (4.1)$$

The probability of reflection at the monochromator is then given by

$$P(\gamma_0, \gamma_1, \Delta k) = P_M \exp\{-\tfrac{1}{2}[\gamma_1/D'_M + \Delta k(\tan\theta_M)/kD'_M]^2\}, \qquad (4.2)$$

where the effective Darwin widths are

$$D'_M = \left(\frac{\tan\theta_M+\tan\psi_M}{\tan\theta_M-\tan\psi_M}\right)^{1/2} D_M. \qquad (4.3)$$

The analysis can then be carried through in exactly the same way as for a symmetrically cut monochromator. In the case of a synchrotron source the relation between γ_0 and γ_1 [(4.1)] shows that the expressions involving the collimation α_0 are altered as well as these involving D_M. The final expressions are considerably more complex than those for symmetrically cut crystals and so will not be given in detail. The general features are, however, that as ψ_M increases the effective resolution elements increase, while if ψ_M is less than 0, and particularly as it approaches the limiting case of $-\theta_M$, the resolution elements tend to zero and the spectrometer has much improved resolution but a very low intensity.

Double monochromators

Double monochromators (Fig. 11*a*) are useful because the wavelength can then be scanned while keeping the sample in a constant position. Within the Gaussian approximation, which is appropriate for mosaic crystals, the effect of a non-dispersive double monochromator with no collimation between the monochromators (Fig. 11*a*) is that the probability is the product of the probability of the two monochromators. This is then equivalent to an effective mosaic spread

$$\eta_M^2 = [(1/\eta_{M_1})^2+(1/\eta_{M_2})^2]^{-1}.$$

Within the Gaussian approximation a similar result can be obtained for perfect crystals with

$$D_M^2 = [(1/D_{M_1})^2+(1/D_{M_2})^2]^{-1}.$$

The effect on the resolution produced by a double monochromator may be different from this because of the non-Gaussian form of the Darwin curve. In particular, because the central part of the Darwin function for non-absorbing crystals is more square-topped than a Gaussian, the effective Darwin width of the double monochromator may be larger than obtained by the convolution of two Gaussians. Secondly, and in contrast, the long tails of the Darwin

function are cut off much more rapidly by the double monochromator, so the Gaussian approximation may well be a better approximation for a double monochromator than for a single monochromator.

Finally, we discuss the case of a dispersive double monochromator (Fig. 11*b*), or, in practice, the double-double monochromator of Fig. 11(*c*). The results for mosaic crystals are the simple convolution of the Gaussian forms for each of the individual crystals, giving the same forms but with a different effective mosaic spread. With two identical perfect crystals the result for the probability function of a dispersive double monochromator is

$$P(\gamma_0, \gamma_1, \Delta k) = P_M^2 \exp\left(-\{\tfrac{1}{2}(\gamma_1/D_M)^2 + [\Delta k\,(\tan\theta_M)/kD_M]^2\}\right), \qquad (4.4)$$

where D_M is the Darwin width of the single monochromator divided by $\sqrt{2}$. This alters the resolution from the expressions given earlier. In particular, the monochromator term in A' [(2.11), (2.15) and (2.17)] becomes

$$[(\tan\theta_M)^2 + (\tan\theta)^2]/D_M^2,$$

and the expressions for the resolution matrix elements are

$$\begin{aligned} M_{11}^x &= [(\tan^2\theta_A)/D_A^2 \\ &\quad + (1/D_M^2 + 1/D_A^2)\tan^2\theta_M]/D_M^2 \\ M_{12}^x &= (\tan^2\theta_M + \tan^2\theta_A - 2\tan\theta_A\tan\theta)/D_M^2 D_A^2 \\ &\quad + (\tan^2\theta_M)/D_M^4 \qquad (4.5) \\ M_{22}^x &= (2\tan\theta - \tan\theta_A)^2/D_M^2 D_A^2. \end{aligned}$$

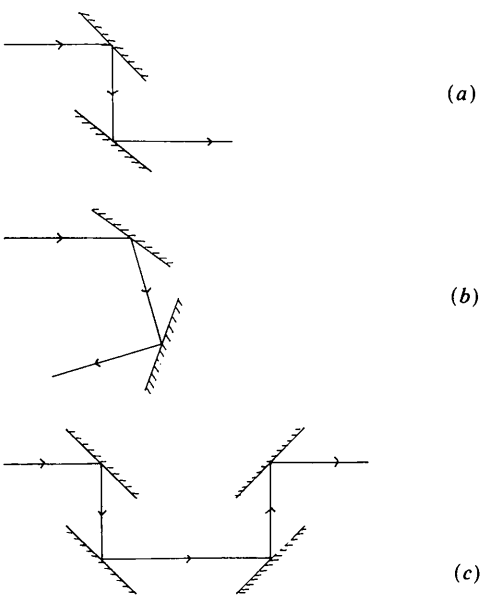

Fig. 11. (*a*) A non-dispersive double monochromator. (*b*) A dispersive double monochromator. (*c*) A four-crystal dispersive monochromator.

The expressions for M_{11}^c, M_{12}^c and M_{22}^c for both a conventional and synchrotron source are unchanged.

The main effect of the double monochromator in comparison with the results for a symmetric diffractometer with a single monochromator occurs when $\theta_M = \theta_A$, because in this case M_{11}^x and M_{12}^x are zero and the resolution elements are controlled by α_0 or σ. This does not occur with the dispersive monochromator, because M_{11}^x and M_{12}^x are then generally non-zero and the resolution is correspondingly greatly improved. With a single monochromator M_{22}^x is zero in the focusing condition when $2\tan\theta = \tan\theta_A + \tan\theta_M$. With a dispersive double monochromator this condition is replaced by $2\tan\theta = \tan\theta_A$. The use of a dispersive double monochromator improves the resolution of the instrument, but this is coupled to a corresponding reduction in the intensity.

Bent monochromators and focusing mirrors

Bent monochromators and mirrors are frequently used in experiments to focus the X-ray beam onto small samples. Within the limits of our treatment of the resolution function, a bent monochromator is equivalent to a mosaic monochromator with a mosaic spread determined by the bend of the monochromator. The difference between a bent crystal and a mosaic crystal, apart from an improvement in the efficiency P_M, is that the bent crystal reflects only those rays which will be incident on a small sample, whereas the mosaic crystal reflects rays which will be incident on a much larger area. This may be very important in optimizing the intensity but the resolution is given by the formalism developed above for mosaic crystals.

A similar effect occurs for a focusing mirror before the monochromator. This usually focuses the beam so that small samples can be used, but within the limitations of our formalism its effect can be incorporated in the pre-monochromator collimation α_0 and β_0.

5. Summary and discussion

Triple-crystal X-ray diffractometers are essential for high-resolution studies of the X-ray scattering to study phase transitions, interfaces and surfaces. If the instruments are operated so that the properties of the monochromator and analyser determine the resolution, as is usually the case, the resolution function can then be evaluated in detail and the expressions are given in § 2. These are the main results of this paper and are useful for the interpretation of experimental results and for the optimization of experiments. The expressions are derived both for a conventional source where the resolution is determined by the line width of the characteristic line, and for a continuous synchrotron source where it is deter-

mined by the pre-monochromator collimation or emittance of the synchrotron. The main approximation made in the derivations is the Gaussian approximation. This is certainly satisfactory for mosaic monochromators or analysers, and is at least a reasonable approximation for perfect crystals close to the centre of the resolution function. The effects of non-Gaussian tails are important in some experiments, as discussed, for example, by Ryan (1986).

One aspect of the results which has not been considered is the effect for a conventional source of a doublet such as Cu $K\alpha_1$ and $K\alpha_2$. The effect of this and its elimination has been discussed (Ryan, 1986) and the splitting between the peaks along $\mathbf{Q}_0$ is illustrated in Fig. 5. Clearly this splitting is much smaller than the longitudinal resolution Δ_x for small $\mathbf{Q}_0$ and with a graphite monochromator and analyser, but at large $\mathbf{Q}_0$ the resolution function will be two-peaked. This is clearly undesirable and resolution corrections are most readily made under conditions in which the $K\alpha_1$ and $K\alpha_2$ beams can be separated.

In § 3 we discussed the effect of the analyser on measurements of the intensity. We were able to show that for samples with zero mosaic spread the intensity is simply dependent upon the angles if the intensity is measured by varying the wave-vector transfer parallel to $\mathbf{Q}_0$ through the Bragg reflection. Any other path gives results which are a complicated function of the angle of scattering and of the resolution, and these effects are illustrated in Figs. 9 and 10. An alternative, and in practice the only satisfactory approach for mosaic crystals, is a two-dimensional scan of the wave vector over the Bragg reflection to give an adequate measure of the structure. In both cases, however, corrections for thermal diffuse scattering *etc.* must be re-evaluated.

Similar considerations apply to the measurement of the intensity of rods of scattering from surfaces and interfaces. The intensities are best measured by scanning the wave vector perpendicular to the rods to obtain the integrated intensity. This is then directly proportional to the scattering power of the rod.

Although the resolution was evaluated with the assumption that the monochromator was a single monochromator, the formalism is readily extended to cope with double monochromators and asymmetrically cut monochromators. It is hoped that the expressions derived above will be useful in the interpretation of experimental results. We are planning a series of measurements to test the formalism and the usefulness of the Gaussian approximation for the central part of the resolution function and the results will be published in due course.

I am grateful for many discussions of the resolution of triple-crystal diffractometers with T. Ryan, R. J. Nelmes, P. J. Mitchell and S. Bates. Financial support was provided by the Science and Engineering Research Council.

References

ANDREWS, S. R. & COWLEY, R. A. (1985). *J. Phys. C*, **18**, 6427–6439.
ANDREWS, S. R. & COWLEY, R. A. (1986). *J. Phys. C*, **19**, 615–635.
AXE, J. D. & HASTINGS, J. B. (1983). *Acta Cryst.* A**39**, 593–594.
BJERRUM-MØLLER, H. & NIELSEN, M. (1970). *Instrumentation for Neutron Inelastic Scattering Research*, pp. 49–76. Vienna: International Atomic Energy Agency.
CHESSER, N. J. & AXE, J. D. (1973). *Acta Cryst.* A**29**, 160–169.
COOPER, M. J. & NATHANS, R. (1967). *Acta Cryst.* **23**, 357–367.
COWLEY, R. A. & RYAN, T. (1987). *J. Phys. D*, **20**, 61–68.
PYNN, R., FUJII, Y. & SHIRANE, G. (1983). *Acta Cryst.* A**39**, 38–46.
ROBINSON, I. K. (1986). *Phys. Rev. B*, **33**, 3830–3836.
ROBINSON, I. K., WASKIEWICZ, W. K., TENG, R. T. & BOHR, J. (1986). *Phys. Rev. Lett.* **57**, 2714–2717.
RYAN, T. (1986). PhD Thesis. Edinburgh Univ., Scotland.
STEDMAN, R. (1968). *Rev. Sci. Instrum.* **39**, 878–883.
ZACHARIASEN, W. H. (1945). *Theory of X-ray Diffraction in Crystals*. New York: Wiley.

International Union of Crystallography

Acta Cryst. (1987). A**43**, 836–838

International Tables for Crystallography Volume A: *Space-Group Symmetry*

Second, revised edition

The second, revised edition of *International Tables for Crystallography*, Volume A: *Space-Group Symmetry* (1987) has recently been published by D. Reidel Publishing Company, PO Box 17, 3300 AA Dordrecht, The Netherlands. The present edition is considerably revised and new material has been added. Improvements include: new diagrams for the 17 plane groups and for the 25 trigonal space groups; the incorporation of two new sections, 8.3.6 and 15, on normalizers of space groups; and a revised *Subject Index*. All changes and additions are detailed in the 'Foreword to the Second, Revised Edition'.

A number of errors were found in the first edition and a list of errata is given below. These errata and the pagination used refer to the First Edition (1983) and to the Reprinted First Edition (1984) and are in addition to those published in *Acta Cryst.* (1984), A**40**, 485. All errata, except those marked, have been corrected in the Second, Revised Edition (1987).

Purchasers of the first edition may obtain free reprints of the new sections 8.3.6 and 15 from The Technical Editor, International Union of Crystallography, 5 Abbey Square, Chester CH1 2HU, England.